Novel (ovario) leukodystrophy related to *AARS2* mutations

Cristina Dallabona, PhD*
Daria Diodato, MD*
Sietske H. Kevelam, MD*
Tobias B. Haack, MD, PhD
Lee-Jun Wong, PhD
Gajja S. Salomons, PhD
Enrico Baruffini, PhD
Laura Melchionda, MSc
Caterina Mariotti, MD
Tim M. Strom, PhD
Thomas Meitinger, PhD
Holger Prokisch, PhD
Kim Chapman, MD
Alison Colley, MD
Helena Rocha, MD
Katrin Őunap, MD
Raphael Schiffmann, MD
Ettore Salsano
Mario Savoiardo, MD†
Eline M. Hamilton, MD
Truus E. M. Abbink, PhD
Nicole I. Wolf, MD
Ileana Ferrero, PhD
Costanza Lamperti, MD, PhD
Massimo Zeviani, MD, PhD
Adeline Vanderver, MD‡
Daniele Ghezzi, PhD‡
Marjo S. van der Knaap, MD‡

Correspondence to
Dr. van der Knaap:
ms.vanderknaap@vumc.nl
or Dr. Ghezzi:
dghezzi@istituto-besta.it

Supplemental data at Neurology.org

ABSTRACT

Objectives: The study was focused on leukoencephalopathies of unknown cause in order to define a novel, homogeneous phenotype suggestive of a common genetic defect, based on clinical and MRI findings, and to identify the causal genetic defect shared by patients with this phenotype.

Methods: Independent next-generation exome-sequencing studies were performed in 2 unrelated patients with a leukoencephalopathy. MRI findings in these patients were compared with available MRIs in a database of unclassified leukoencephalopathies; 11 patients with similar MRI abnormalities were selected. Clinical and MRI findings were investigated.

Results: Next-generation sequencing revealed compound heterozygous mutations in *AARS2* encoding mitochondrial alanyl-tRNA synthetase in both patients. Functional studies in yeast confirmed the pathogenicity of the mutations in one patient. Sanger sequencing revealed *AARS2* mutations in 4 of the 11 selected patients. The 6 patients with *AARS2* mutations had childhood- to adulthood-onset signs of neurologic deterioration consisting of ataxia, spasticity, and cognitive decline with features of frontal lobe dysfunction. MRIs showed a leukoencephalopathy with striking involvement of left-right connections, descending tracts, and cerebellar atrophy. All female patients had ovarian failure. None of the patients had signs of a cardiomyopathy.

Conclusions: Mutations in *AARS2* have been found in a severe form of infantile cardiomyopathy in 2 families. We present 6 patients with a new phenotype caused by *AARS2* mutations, characterized by leukoencephalopathy and, in female patients, ovarian failure, indicating that the phenotypic spectrum associated with *AARS2* variants is much wider than previously reported.
***Neurology*® 2014;82:1–9**

GLOSSARY

AARS2 = alanyl-tRNA synthetase 2; **LBSL** = leukoencephalopathy with brainstem and spinal cord involvement and lactate elevation; **OMIM** = Online Mendelian Inheritance in Man; **tRNA** = transfer RNA; **WES** = whole-exome sequencing.

Mutations in genes coding for mitochondrial aminoacyl transfer RNA (tRNA) synthetases, the enzymes that charge a specific tRNA with its cognate amino acid, are recently emerging as a new important cause of mitochondrial disease and have been associated with a wide spectrum of clinical phenotypes.[1–3] However, defects in each aminoacyl tRNA synthetase seem to determine rather homogeneous clinical presentations.[1–5]

*These authors share first authorship.

‡These authors share senior authorship.

†Deceased.

From the Department of Life Sciences (C.D., E.B., I.F.), University of Parma; Unit of Molecular Neurogenetics (D.D., L.M., C.L., D.G.), SOSD Genetics of Neurodegenerative and Metabolic Diseases (C.M.), and Departments of Clinical Neurosciences (E.S.) and Neuroradiology (M.S.), Fondazione Istituto Neurologico Carlo Besta, Istituto di Ricovero e Cura a Carattere Scientifico, Milan, Italy; Department of Child Neurology (S.H.K., E.M.H., T.E.M.A., N.I.W., M.S.v.d.K.), Department of Clinical Chemistry, Metabolic Unit (G.S.S.), Neuroscience Campus Amsterdam, and Department of Functional Genomics, Center for Neurogenomics and Cognitive Research (M.S.v.d.K.), VU University Medical Center, Amsterdam, the Netherlands; Institute of Human Genetics (T.B.H., T.M.S., T.M., H.P.), Technical University, Munich; Institute of Human Genetics (T.B.H., T.M.S., T.M., H.P.), Helmholtz Zentrum Munich, Neuherberg, Germany; Department of Molecular and Human Genetics (L.-J.W.), Baylor College of Medicine, Houston, TX; Department of Genetics (K.C.), and Center for Genetic Medicine Research, Department of Neurology (A.V.), Children's National Medical Center, Washington, DC; Department of Clinical Genetics (A.C.), Liverpool Hospital, Sydney, Australia; Neurology Department (H.R.), Centro Hospitalar São João, and Department of Clinical Neuroscience and Mental Health, Faculty of Medicine, University of Porto, Portugal; Medical Genetics Center (K.Ő.), United Laboratories, Tartu University Clinics, Estonia; Institute of Metabolic Disease (R.S.), Baylor Research Institute, Dallas, TX; and Mitochondrial Biology Unit–MRC (M.Z.), Cambridge, UK.

Go to Neurology.org for full disclosures. Funding information and disclosures deemed relevant by the authors, if any, are provided at the end of the article.

The use of whole-exome sequencing (WES) has markedly increased efficiency and improved genetic analysis for inherited disorders, allowing gene identification for small groups of patients sharing a phenotype, individual cases with atypical presentation, and disorders lacking consistent genotype-phenotype correlation.[6–8]

Mutations in the mitochondrial alanyl-tRNA synthetase 2 gene (*AARS2*; OMIM *612035) have been found in severe infantile cardiomyopathy in 2 families.[9] In the present study, we describe a very different clinical picture determined by *AARS2* genetic defects in 6 patients affected by a progressive leukoencephalopathy and, in females, ovarian failure, a clinical presentation previously described as "ovarioleukodystrophy."[10]

METHODS Standard protocol approvals, registrations, and patient consents. The study was approved by the Ethical Committees of the Istituto Neurologico Besta, Milan, Italy; the Children's National Medical Center, Washington, DC; and the VU University Medical Center, Amsterdam, the Netherlands, in agreement with the Declaration of Helsinki. Informed consent was signed by the patients.

Patients. Patients 1 (P1) and 2 (P2) were included in 2 independent next-generation sequencing studies. On the basis of the MRI findings in these 2 patients, we selected 10 patients from 9 families from the Amsterdam database, which contains more than 3,000 cases with an unclassified leukoencephalopathy[11] and one patient from the leukoencephalopathy cases of the Istituto Neurologico Besta without genetic diagnosis. Common MRI features were frontal and parietal white matter abnormalities with relative sparing of the central posterior-frontal or frontoparietal region. The anterior part of the corpus callosum and a thin strip in the splenium were affected, with relative sparing of the central region. Most female patients had ovarian failure in addition to the leukoencephalopathy. We also included 2 patients with unsolved ovarioleukodystrophy, in whom no mutations in *EIF2B1–5* had been found.[10,12] For all patients, we collected clinical and laboratory data retrospectively. We analyzed available MRIs, as described.[10]

Molecular studies. We extracted genomic DNA by standard methods from leukocytes or muscle biopsies. In P1, we performed WES and variant filtering, as described.[13] For P2, we used a custom probe library for target gene capture (Roche NimbleGen Inc., Madison, WI) designed to capture coding exons plus 20 base pairs into the flanking introns of 500 genes known to be related to mitochondrial disorders, followed by deep sequencing at average coverage depth of 1,000 per base. Because of rapid clinical deterioration of P2, we also initiated clinical WES (Illumina, San Diego, CA). We performed Sanger sequencing of the gene identified by WES in all patients.[9]

Functional studies. We used yeast strains derived from W303-1B.[14] Detailed methods including respiratory activity, cytochrome spectra, in vivo mitochondrial DNA protein synthesis, aminoacylation of mitochondrial tRNA for alanine, cytochrome *c* oxidase (complex IV) and complex I + III activities, and primers for the preparation of plasmids used in this study are reported in the e-Methods and table e-1 on the *Neurology*® Web site at Neurology.org.

RESULTS Patients and laboratory findings. The clinical features of the patients in whom we found mutations in the gene mentioned below are summarized in table e-2. Herein, we give a brief description.

P1 is a female in whom developmental delay became evident at 2 years of age. She achieved walking without support at 3, but with impaired balance. Her condition remained stable until age 15, when she developed progressive gait ataxia, tremor, cognitive deterioration, and psychosis. At age 18, she developed secondary amenorrhea due to ovarian failure. The latest neurologic examination at age 30 revealed severe cerebellar ataxia with nystagmus, dysarthria, intention tremor, and instable gait. She could walk with support. General physical examination revealed no abnormalities and no evidence of cardiac dysfunction. ECG and cardiac ultrasound were normal.

P2 is a male who came to medical attention in infancy because of congenital nystagmus. In primary school, mild clumsiness and learning difficulties were a concern. In his early teenage years, he developed mild right-sided hemiparesis and ataxia, which was ascribed to periventricular leukomalacia due to periventricular white matter abnormalities on MRI. Around age 17, deterioration set in with bilateral dystonia and spasticity, dysarthria, and cognitive decline. A viral gastroenteritis was followed by abrupt mental decline, unintelligible speech, inability to eat due to choking, recurrent vomiting, and inability to walk because of worsening of ataxia and spasticity, left more than right. General physical examination revealed no abnormalities and no evidence for cardiac dysfunction.

P3 is a female who presented with secondary amenorrhea due to ovarian failure at age 28. At age 33, she developed depression, cognitive deterioration, behavioral problems with signs of frontal dysfunction, and urinary incontinence. Neurologic examination revealed downbeat nystagmus and some postural and appendicular tremor of the arms, but otherwise no motor disability. She developed stereotyped motor behavior and severe apraxia. At age 35, she did not recognize family members anymore. She had to be tube fed. Antiepileptic medication was started because of epileptic seizures. At age 36, she was bedridden and had no interactions with her surroundings.

P4 is a female who was diagnosed with ovarian failure at age 23 years. She developed tremor of her hands at age 24. Because of white matter abnormalities on MRI, she was diagnosed with multiple sclerosis. From age 26, rapid cognitive, behavioral, and motor deterioration became evident. She developed

progressive dystonia, cerebellar ataxia, and spasticity, left more than right. General physical examination revealed no abnormalities. She lost speech, became bedridden, and died at age 28.

P5 is a female who had primary amenorrhea due to ovarian failure. From age 40, she developed depression and rapid cognitive deterioration. Neurologic examination revealed no motor dysfunction. General physical examination revealed no abnormalities. She became bedridden and died at age 46.

P6 is a female who was diagnosed with ovarian failure at 20 years of age. At age 22, she presented with gait problems caused by hypertonia of the legs, left more than right. She developed depression but no cognitive regression. Neurologic examination revealed a spastic paraparesis with ataxic signs. The disease was rapidly progressive. At latest examination at age 25, she was wheelchair-bound.

Laboratory findings are summarized in table e-3. None of the patients had elevated blood or CSF lactate. All 5 female patients had primary or secondary amenorrhea due to ovarian failure.

P1 and P6 were the only patients extensively investigated for a possible mitochondrial defect. In P1, the Gomori trichrome stain and succinate dehydrogenase reaction of a skeletal muscle biopsy were normal, whereas the histochemical reaction to cytochrome *c* oxidase was diffusely reduced (figure 1A). Likewise, biochemical assay showed severe isolated cytochrome *c* oxidase deficiency (15% of residual activity) in muscle homogenate (figure 1B), whereas the activities of all respiratory chain complexes, including cytochrome *c* oxidase, were normal in fibroblasts. Oxygraphic studies performed in patients' fibroblasts, grown in either glucose or galactose medium, showed no defect (not shown). Sequencing of mitochondrial DNA revealed a heteroplasmic variant with a low level of mutation load: m.5979G>A (p.Ala26Thr) in *MTCO1*, reported as a rare single nucleotide polymorphism (<0.1% in Mitomap database) present in haplogroup H45 and deemed not pathogenic. In P6, histologic and histochemical analyses of muscle biopsy revealed diffusely reduced cytochrome *c* oxidase staining, but no ragged red fibers. Measurement of individual oxidative phosphorylation enzyme activities in muscle homogenate showed reduced cytochrome *c* oxidase (33% of residual activity) (figure 1B). Mitochondrial DNA sequencing revealed no pathogenic point mutations, but several polymorphisms typical of haplogroup T1a1.

MRI abnormalities. The MRI abnormalities are summarized in table e-4 and illustrated in figures 2 and e-1. In all 6 patients, the cerebral white matter abnormalities were inhomogeneous and patchy, affecting and sparing strips of tissue. In several patients, the signal of small parts of the T2-hyperintense white matter was low on fluid-attenuated inversion recovery images, indicating white matter rarefaction. Typically, the signal abnormalities were predominantly present in the frontal and parietal periventricular and deep white matter, sparing a segment of white matter in between. White matter structures were affected in a tract-like manner, with involvement of left-right connections through the corpus callosum and involvement of descending connections. Depending on the location of the cerebral hemispheric white matter abnormalities, the frontopontine, pyramidal, or parieto-occipitopontine tracts were longitudinally affected. The corpus callosum abnormalities were also dependent on the cerebral hemispheric white matter involvement; they could be limited to a single lesion in the splenium, affect a large part of the anterior corpus callosum and only a narrow strip in the splenium, or involve the entire corpus callosum in an inhomogeneous manner. Diffusion-weighted images showed multiple small areas of restricted diffusion in the cerebral white matter and corpus callosum. The abnormalities were limited to white matter structures and were progressive over time. No contrast enhancement was observed. Cerebellar atrophy was variable and affected the vermis more than the hemispheres. Cerebral atrophy was at most mild.

WES and Sanger sequencing. We performed WES on genomic DNA from P1.[6] After excluding common single nucleotide polymorphisms (>0.1%), we prioritized the remaining changes according to the presence of homozygous or compound heterozygous mutations, as expected for a recessive inherited trait, and for known or predicted mitochondrial localization of the corresponding protein.[15] This filtering led to the identification of a single outstanding gene entry, *AARS2* (NC_000006.11), in which a missense (c.149T>G, p.Phe50Cys) and a nonsense (c.1561C>T, p.Arg521*) heterozygous variant were present (NM_020745.3) (figure 1C, table 1), segregating within the family.

We subjected P2 to a gene panel containing 500 genes known to cause mitochondrial disorders and to clinical WES. With both policies, we identified 2 missense mutations in *AARS2* (c.2893G>A, p.Gly965Arg and c.1213G>A, p.Glu405Lys).

We performed Sanger sequencing of *AARS2* exons and intron-exon boundaries in all patients and found *AARS2* mutations in 4 of the 11 patients selected on the basis of MRI features (table 1). We did not find *AARS2* mutations in the 2 patients with ovarioleukodystrophy. All identified nucleotide substitutions with a frequency <0.01% in public databases correspond to amino acid changes predicted to be deleterious (tables 1 and e-5).

Functional studies. Because no biochemical readout was detected in cell lines of P1, we tested the possible deleterious impact of the *AARS2* mutations on oxidative

Figure 1 Biochemical and genetic features

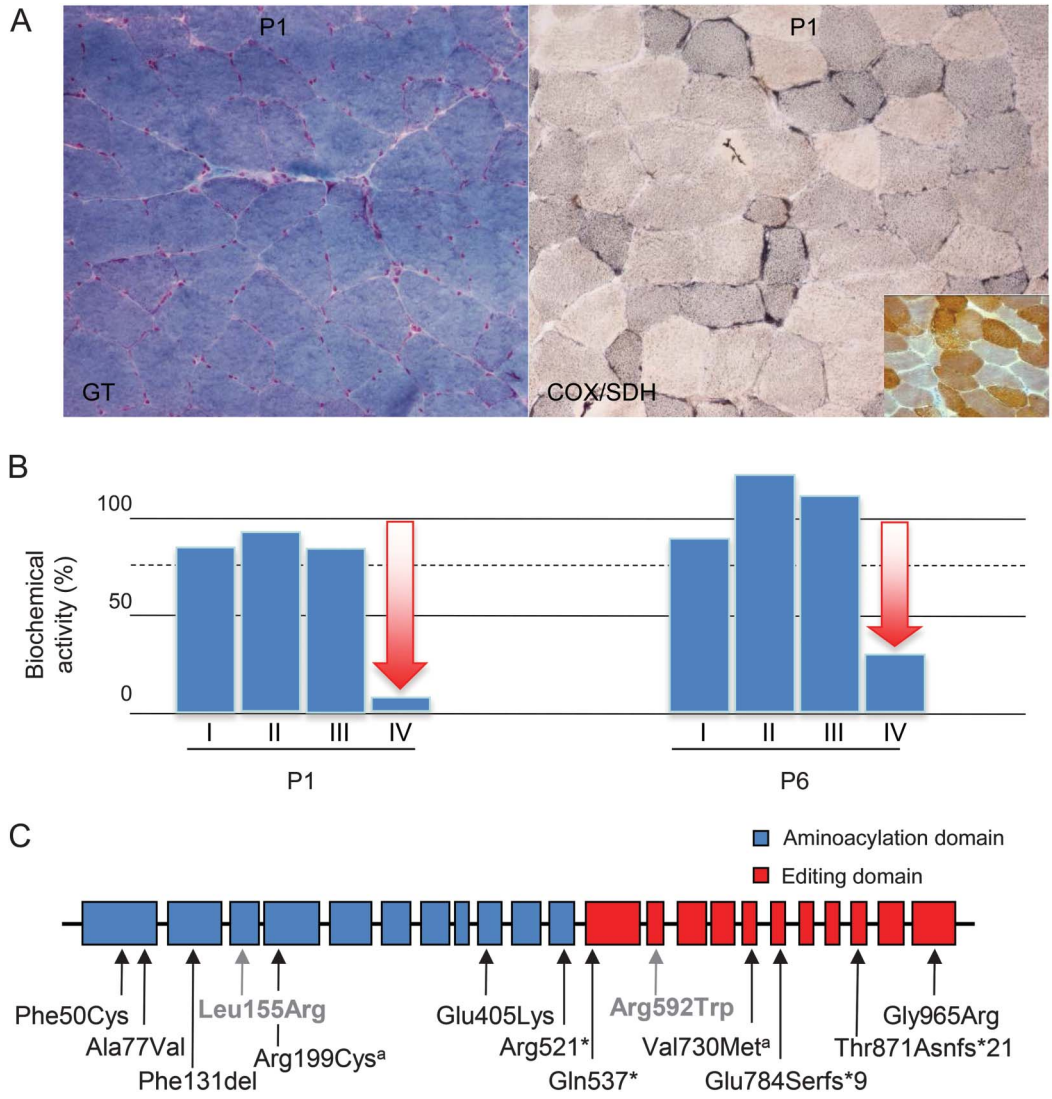

(A) Morphologic analysis of muscle biopsy from patient P1: Gomori trichrome (GT) staining and cytochrome *c* oxidase (COX)/succinate dehydrogenase (SDH) histoenzymatic double staining (COX/SDH). Inset shows the reaction in an age-matched control biopsy. (B) Biochemical activities of mitochondrial respiratory chain complexes in patients P1 and P6 muscle homogenates. All enzymatic activities are normalized for citrate synthase activity and indicated as percentages relative to the mean control value. (C) Genomic structure of *AARS2* with exons coding for the aminoacylation (blue) and editing (red) domains. The arrows indicate the position of mutations identified in this study (black) or previously reported (gray). [a]The 2 missense variants p.Arg199Cys and p.Val730Met are on the same allele; the latter (rs35623954) is reported to have a frequency >1% in control populations, suggesting that the former is the pathogenic variant.

phosphorylation in a *Saccharomyces cerevisiae* yeast model. Phe50 in human *AARS2* is highly conserved in phylogenesis, including yeast (figure e-2), in which the ortholog *ala1* gene (NC_001147.6) codes for both the cytosolic and mitochondrial alanyl tRNA synthetase.[16] We disrupted *ala1* by homologous recombination and re-expressed the wild-type cytosolic isoform (supplemental data), thus generating a viable but oxidative phosphorylation–incompetent strain ($ala1^{L\text{-}16X}$), which lacked the mitochondrial isoform. In this strain, we expressed either the wild-type *ala1* gene ($ala1^{wt}$), a p.Phe22Cys mutant allele ($ala1^{F22C}$), equivalent to the human p.Phe50Cys variant, or a p.Val500* mutant allele ($ala1^{V500X}$), equivalent to the human p.Arg521* variant.

In contrast to $ala1^{wt}$, the expression of ala^{V500X} failed to restore growth on nonfermentable sources (i.e., glycerol). The oxidative growth of the strain expressing $ala1^{F22C}$ was similar to the wild-type at 28°C but reduced at 37°C (figure e-3). We obtained similar results from assays evaluating the oxygen consumption (figure 3A), the in vivo mitochondrial protein synthesis (figure 3B), the activities of the respiratory chain complexes I + III and IV, and the spectra of mitochondrial respiratory chain cytochromes (figure e-3). Finally, we evaluated the

Figure 2 Brain MRI

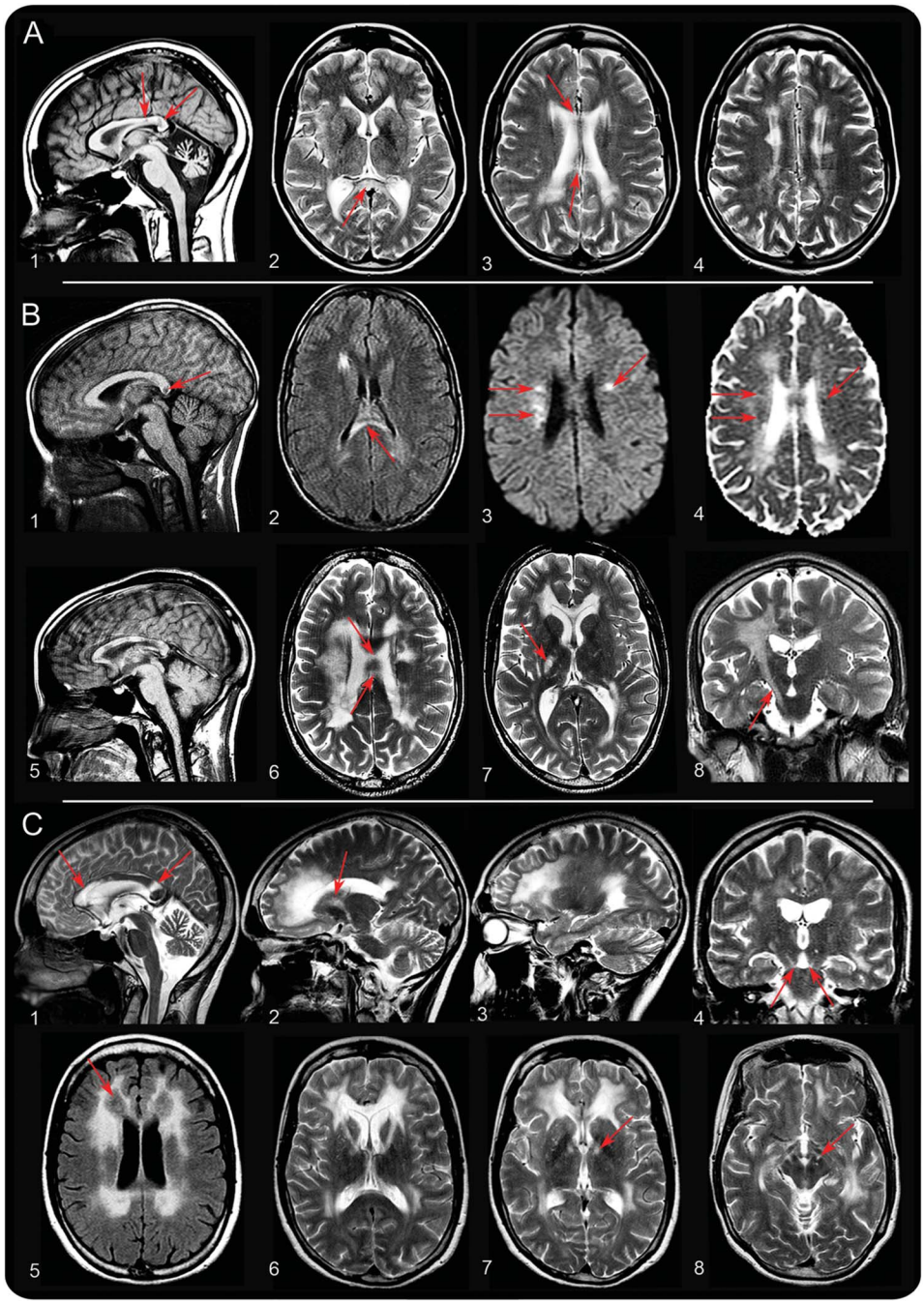

(A) MRI in P1 at age 28. The sagittal T1-weighted image shows serious cerebellar atrophy and 2 strips of abnormal signal in the splenium (arrows in image 1). The axial T2-weighted images show inhomogeneous areas of abnormal signal in the periventricular white matter. The areas on the left and right are connected signal abnormalities in the corpus callosum (arrows in images 2–4). (B) MRI in P2 at age 14 (images 1 and 2), age 21 (images 3 and 4), and age 23 (images 5–8). At age 14, a lesion is seen in the splenium of the corpus callosum (arrow in image 1) and in the right frontal periventricular white matter. The diffusion-weighted images suggest the presence of multiple small areas of restricted diffusion in the abnormal white matter (arrows in image 3), confirmed by low signal of the corresponding areas on the apparent diffusion coefficient map (arrows in image 4). The most recent MRI shows multiple segments of abnormal signal in the corpus callosum (image 5 and arrows in image 6). More extensive signal abnormalities are seen in the periventricular white matter, especially on the right (images 6 and 7). Signal abnormalities extend downward through the posterior limb of the internal capsule and the pyramidal tracts in the brainstem on the right (arrows in images 7 and 8). (C) MRI in patient 3 at age 35. The midsagittal image shows that the anterior part of the corpus callosum is abnormal, whereas only a strip of signal abnormality is seen in the splenium (arrows in image 1). Images 2 and 3 illustrate that the frontal and parietal white matter is abnormal, whereas the central white matter in between is normal. The tract involvement is evident (arrows in images 2 and 4). The axial fluid-attenuated inversion recovery image shows that the affected white matter is rarefied (arrow in image 5). The axial T2-weighted images illustrate the involvement of the anterior limb of the internal capsule (image 6) and the frontopontine tracts going down into the brainstem (arrows in images 7 and 8).

Table 1 *AARS2* mutations found in the patients

Patient	cDNA	Protein	State	Paternal/maternal	EVS frequency, %[a]
1	c.149T>G	p.Phe50Cys	Heterozygous	M	ø
	c.1561C>T	p.Arg521*	Heterozygous	P	ø
2	c.2893G>A	p.Gly965Arg	Heterozygous	M	ø
	c.1213G>A	p.Glu405Lys	Heterozygous	P	ø
3	c.1609C>T and c.2350del	p.Gln537* and p.Glu784Serfs*9	Heterozygous	M	ø
	c.595C>T and c.2188G>A	p.Arg199Cys and p.Val730Met	Heterozygous	P	0.008 and 3.1
4	c.230C>T	p.Ala77Val	Heterozygous	M	0.008
	c.595C>T and c.2188G>A	p.Arg199Cys and p.Val730Met	Heterozygous	P	0.008 and 3.1
5	c.595C>T and c.2188G>A	p.Arg199Cys and p.Val730Met	Heterozygous	M	0.008 and 3.1
	c.390_392del	p.Phe131del	Heterozygous	P	ø
6	c.595C>T and c.2188G>A	p.Arg199Cys and p.Val730Met	Heterozygous	M	0.008 and 3.1
	c.2611dup	p.Thr871Asnfs*21	Heterozygous	P	ø

Abbreviations: cDNA = complementary DNA; EVS = Exome Variant Server (varianttools.sourceforge.net/Annotation/EVS).
[a] Ø = not found.

charging of the tRNA with alanine; the p.Val500* change determined the complete inability to charge mitochondrial $tRNA^{Ala}$ with its cognate amino acid, whereas the p.Phe22Cys change determined a partial reduction in the amino acid charging at 37°C (figure 3C). We analyzed the effects of $ala1^{L125R}$, corresponding to p.Leu155Arg,[9] and found that in all experiments this missense mutation behaves as a null allele (figures 3 and e-3). The other known *AARS2* mutation, p.Arg592Trp,[9] could not be tested, because the residue is not conserved in yeast (figure e-2).

The above yeast experiments confirmed that the p.Phe50Cys missense mutation is deleterious only in stress conditions, whereas the truncated protein due to the nonsense mutation is nonfunctional.

DISCUSSION Defects in several different mitochondrial aminoacyl tRNA synthetases have been associated with specific clinical phenotypes.[1,3–5] However, these enzymes are ubiquitously expressed and take part in the same process, so this phenotypic segregation is difficult to explain. This conclusion of phenotypic segregation may be based on inclusion bias, because the genes are only analyzed in patients with specific phenotypes. In addition, the number of patients with mutations in different mitochondrial aminoacyl tRNA synthetases is at present too small to provide conclusive evidence of the existence of exclusive genotype-phenotype correlations.

Recently, *AARS2* mutations have been reported in 3 subjects as the cause for infantile hypertrophic cardiomyopathy, lactic acidosis, and brain and skeletal muscle involvement, with early fatal outcome.[9] In contrast, our patients have later-onset neurologic dysfunction due to a leukoencephalopathy and no signs of cardiomyopathy. In P1 and P2, onset was in childhood and initially followed a stable course or very slow disease progression. In all cases, the course after onset of evident deterioration was rather rapid. The neurologic dysfunction comprised motor deterioration, consisting of cerebellar ataxia and spasticity, and cognitive decline with features of frontal lobe dysfunction with poor memory, inactivity and other behavioral changes, as well as depression and other psychiatric features. Comparing clinical and MRI findings, it is clear that the clinical signs of the patients depend on which tracts are affected. P2, P4, and P6 had prominent signs of motor dysfunction and had pyramidal tract involvement on MRI. P3 and P5 mainly had signs of behavioral and cognitive dysfunction and frontopontine tract involvement. The striking white matter tract involvement and presence of spots of restricted diffusion in the cerebral white matter are features shared by another disorder with mutations in a mitochondrial aminoacyl tRNA synthetase: "leukoencephalopathy with brainstem and spinal cord involvement and lactate elevation" (LBSL), caused by mutations in *DARS2* (OMIM *610956). In LBSL, the white matter spots of restricted diffusion are ascribed to myelin vacuolization, a feature frequently seen in mitochondrial leukoencephalopathies.[17]

In P1 and P6, we detected a profound, isolated defect of complex IV activity, rather than a combination of mitochondrial DNA–related respiratory chain defects, which is the expected consequence of reduced mitochondrial protein synthesis. The pathogenicity of the 2 *AARS2* variants of P1 was proven in a recombinant yeast model. Of note, the yeast p.Phe22Cys mutation, equivalent to p.Phe50Cys found in P1, impairs complex IV activity much more than

Figure 3 Yeast studies

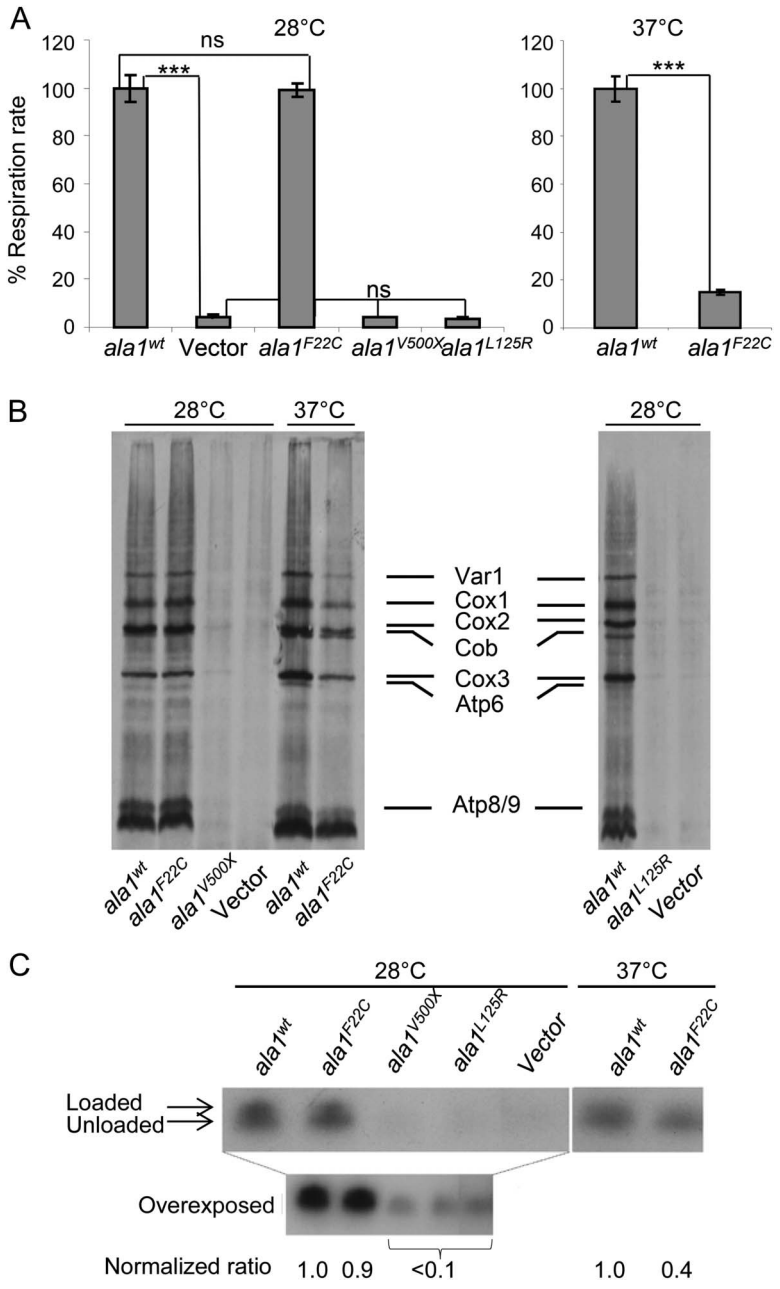

(A) Oxygen consumption rate of the *ala1*$^{L\text{-}16X}$ strain transformed with the *ala1*^{wt} allele, the empty vector, and the mutant alleles *ala1*^{F22C}, *ala1*^{V500X}, and *ala1*^{L125R}. Respiratory rates were normalized to the strain transformed with *ala1*^{wt}, in which the respiratory rate was 81.1 nmol min^{-1} mg^{-1} at 28°C and 33.4 nmol min^{-1} mg^{-1} at 37°C. Values are the mean of 3 independent experiments, each with an independent clone. Two-tailed paired t test was applied for statistical significance. ***$p < 0.001$. (B) In vivo mitochondrial protein synthesis of the *ala1*$^{L\text{-}16X}$ strain transformed with the *ala1*^{wt} allele, the empty vector, and the mutant alleles *ala1*^{F22C}, *ala1*^{V500X}, and *ala1*^{L125R}. Mitochondrial gene products were labeled with [^{35}S]-methionine in whole cells in the presence of cycloheximide for 10 minutes at 28°C or 37°C. (C) Mitochondrial tRNA^{Ala} loading of the *ala1*$^{L\text{-}16X}$ strain transformed with the *ala1*^{wt} allele, the empty vector, and the mutant alleles *ala1*^{F22C}, *ala1*^{V500X}, and *ala1*^{L125R}. Signals were quantified with Quantity 1 (Bio-Rad, Hercules, CA). For each strain, the ratio between the charged tRNA^{Ala} and the uncharged one was calculated and normalized to the *ala1*^{wt} strain. Atp = ATP synthase; Cob = cytochrome b; Cox = cytochrome c oxidase; ns = not significant; Var1 = small mitochondrial ribosome subunit.

complex I + III activity, whereas p.Leu125Arg, equivalent to human p.Leu155Arg, a mutation of patients with cardiomyopathy,[9] decreases them both, suggesting that an isolated defect of complex IV may predominantly depend on specific missense mutations, possibly influencing the main target tissue (brain vs heart). Variable involvement of different respiratory chain complexes and different degrees of defective activities have also been reported for different mutations in other aminoacyl tRNA synthetases.[18]

The yeast p.Phe22Cys mutation was only deleterious in stress conditions, while the other tested mutations were highly deleterious in basal conditions, suggesting that the human p.Phe50Cys mutant protein maintains residual activity, which could explain the slow disease of our patient, in contrast to the rapidly fatal outcome of the patients with cardiomyopathy.[9] While our yeast model enabled us to evaluate the p.Leu155Arg mutation, poor conservation between human and yeast precluded the validation of the p.Arg592Trp substitution in patients with cardiomyopathy.[9] The latter mutation could impair editing activity of *AARS2*, leading to increased mistranslation of the alanine codon by serine or glycine.[9] According to this hypothesis, a specific pathogenic mechanism, mistranslation, would lead to cardiomyopathy, while translation deficiency, caused by other aminoacyl tRNA synthetase mutations, is usually not associated with heart damage.[3] Of note, hypertrophic cardiomyopathy occurs in subjects with mutations affecting *MTO1*, encoding an enzyme responsible for tRNA modifications that increase accuracy and efficiency of mitochondrial DNA translation.[19,20]

A striking feature was the presence of ovarian failure in all female patients with *AARS2* mutations. Mutations in 2 other mitochondrial aminoacyl tRNA synthetase encoding genes, namely *HARS2* (OMIM *600783) and *LARS2* (OMIM *604544), have recently been associated with Perrault syndrome, a disorder characterized by ovarian dysgenesis and sensorineural hearing loss. However, Perrault syndrome is genetically heterogeneous; it can also be caused by mutations in *HSD17B4*, encoding a peroxisomal enzyme involved in fatty acid β-oxidation, and mutations in *CLPP*, encoding a mitochondrial endopeptidase. Mutations in *POLG* (OMIM *174763), the gene encoding DNA polymerase-γ for the replication of human mitochondrial DNA, may also lead to premature menopause[21] and ovarian failure.[22]

Of the 7 patients included in the present study who had similar MRI abnormalities but no *AARS2* mutations, 2 were male and 2 were prepubertal females. Of the 3 adult female patients, one had normal menses until put on contraceptive injections, one had a period of 3 years of amenorrhea but recently started menstruating again, and for one the information is

not available. It is therefore not possible to make a definitive conclusion on the presence or absence of ovarian failure in these patients.

The preferential involvement of brain white matter and ovaries is shared by vanishing white matter (OMIM #603896), caused by mutations in any of the 5 genes (*EIF2B1* to *EIF2B5*) encoding subunits of the translation initiation factor eIF2B. Female patients often develop ovarian failure, manifest as primary or secondary amenorrhea.[12] eIF2B impairment leads to a defect in translation initiation for nuclear genes, not affecting translation of the mitochondrial encoded proteins. Hence, even if both *AARS2* and *EIF2B1–5* mutations are likely associated with block or dysregulation of protein synthesis, their targets and site of action (mitochondria vs cytosol) are completely separated and, at present, we have no explanation for the common resulting phenotype. Two patients with ovarioleukodystrophy as well as 7 patients with similar MRI abnormalities had no *AARS2* mutations, suggesting that they have mutations in untranslated regions of the gene or there could be another gene(s) that, when mutated, is associated with the same selective vulnerability.

AUTHOR CONTRIBUTIONS

C.D., D.D., S.H.K., T.B.H., L.-J.W., G.S.S., E.B., L.M., C.M., T.M.S., T.M., H.P., K.C., A.C., H.R., K.Ő., R.S., E.S., M.S., E.M.H., T.E.M.A., N.I.W., I.F., C.L., M.Z., A.V., D.G., and M.S.v.d.K. designed the study, performed experiments, collected and analyzed data. M.Z., A.V., D.G., and M.S.v.d.K. wrote the manuscript. C.D., D.D., S.H.K., T.B.H., L.-J.W., G.S.S., E.B., L.M., C.M., T.M.S., T.M., H.P., K.C., A.C., H.R., K.Ő., R.S., E.S., M.S., E.M.H., T.E.M.A., N.I.W., I.F., and C.L. critically revised the manuscript for important intellectual content.

ACKNOWLEDGMENT

The authors thank the families for their collaboration, Dr. Madalena Pinto, Neurology Department, Centro Hospitalar São João, Porto, Portugal, for her care for patient 3, and Carola van Berkel, Warsha Kanhai, and Matilde Fernandez-Ojeda, Departments of Child Neurology and Clinical Chemistry, Neuroscience Campus Amsterdam, VU University Medical Center, Amsterdam, the Netherlands, for their excellent laboratory assistance.

STUDY FUNDING

This work received financial support from the Italian Ministry of Health (GR2010–2316392); Fondazione Telethon grants GGP11011 and GPP10005; CARIPLO grant 2011/0526; Fondazione Pierfranco e Luisa Mariani; the Italian Association of Mitochondrial Disease Patients and Families (Mitocon); EU Ideas ERC program (AdG-322424); the BMBF-funded German Network for Mitochondrial Disorders (mitoNET 01 GM1113C); the E-Rare project GENOMIT (01GM1207); the Dutch National Funding System (ZonMw TOP grant 91211005); and the Optimix Foundation for Scientific Research. Dr. A. Vanderver was supported by the Myelin Disorders Bioregistry Project. We acknowledge the "Cell lines and DNA Bank of Paediatric Movement Disorders and Neurodegenerative Diseases" of the Telethon Network of Genetic Biobanks (grant GTB12001J) and the EuroBioBank Network.

DISCLOSURE

The authors report no disclosures relevant to the manuscript. Mario Savoiardo is deceased; disclosures are not included for this author. Go to Neurology.org for full disclosures.

Received October 24, 2013. Accepted in final form February 27, 2014.

REFERENCES

1. Rötig A. Human diseases with impaired mitochondrial protein synthesis. Biochim Biophys Acta 2011;1807:1198–1205.
2. Yao P, Fox PL. Aminoacyl-tRNA synthetases in medicine and disease. EMBO Mol Med 2013;5:332–343.
3. Konovalova S, Tyynismaa T. Mitochondrial aminoacyl-tRNA synthetases in human disease. Mol Genet Metab 2013;108:206–211.
4. Scheper GC, van der Klok T, van Andel RJ, et al. Mitochondrial aspartyl-tRNA synthetase deficiency causes leukoencephalopathy with brain stem and spinal cord involvement and lactate elevation. Nat Genet 2007;39:534–539.
5. Steenweg ME, Ghezzi D, Haack T, et al. Leukoencephalopathy with thalamus and brainstem involvement and high lactate "LTBL" caused by EARS2 mutations. Brain 2012;135:1387–1394.
6. Haack TB, Haberberger B, Frisch EM, et al. Molecular diagnosis in mitochondrial complex I deficiency using exome sequencing. J Med Genet 2012;49:277–283.
7. Lamperti C, Fang M, Invernizzi F, et al. A novel homozygous mutation in SUCLA2 gene identified by exome sequencing. Mol Genet Metab 2012;107:403–408.
8. Hanchard NA, Murdock DR, Magoulas PL, et al. Exploring the utility of whole-exome sequencing as a diagnostic tool in a child with atypical episodic muscle weakness. Clin Genet 2013;83:457–461.
9. Götz A, Tyynismaa H, Euro L, et al. Exome sequencing identifies mitochondrial alanyl-tRNA synthetase mutations in infantile mitochondrial cardiomyopathy. Am J Hum Genet 2011;88:635–642.
10. Schiffmann R, Tedeschi G, Kinkel RP, et al. Leukodystrophy in patients with ovarian dysgenesis. Ann Neurol 1997;41:654–661.
11. van der Knaap MS, Breiter SN, Naidu S, et al. Defining and categorizing leukoencephalopathies of unknown origin: MR imaging approach. Radiology 1999;213:121–133.
12. Fogli A, Rodriguez D, Eymard-Pierre E, et al. Ovarian failure related to eukaryotic initiation factor 2B mutations. Am J Hum Genet 2003;72:1544–1550.
13. Mayr JA, Haack TB, Graf E, et al. Lack of the mitochondrial protein acylglycerol kinase causes Sengers syndrome. Am J Hum Genet 2012;90:314–320.
14. Thomas BJ, Rothstein R. Elevated recombination rates in transcriptionally active DNA. Cell 1989;56:619–630.
15. Elstner M, Andreoli C, Ahting U, et al. MitoP2: an integrative tool for the analysis of the mitochondrial proteome. Mol Biotechnol 2008;40:306–315.
16. Tang HL, Yeh LS, Chen NK, et al. Translation of a yeast mitochondrial tRNA synthetase initiated at redundant non-AUG codons. J Biol Chem 2004;279:49656–49663.
17. Steenweg ME, Pouwels PJ, Wolf NI, van Wieringen WN, Barkhof F, van der Knaap MS. Leucoencephalopathy with brainstem and spinal cord involvement and high lactate: quantitative magnetic resonance imaging. Brain 2011;134:3333–3341.
18. Rodenburg RJ. Biochemical diagnosis of mitochondrial disorders. J Inherit Metab Dis 2011;34:283–292.
19. Ghezzi D, Baruffini E, Haack TB, et al. Mutations of the mitochondrial-tRNA modifier MTO1 cause hypertrophic cardiomyopathy and lactic acidosis. Am J Hum Genet 2012;90:1079–1087.

20. Baruffini E, Dallabona C, Invernizzi F, et al. MTO1 mutations are associated with hypertrophic cardiomyopathy and lactic acidosis and cause respiratory chain deficiency in humans and yeast. Hum Mutat 2013;34:1501–1509.
21. Luoma P, Melberg A, Rinne JO, et al. Parkinsonism, premature menopause, and mitochondrial DNA polymerase gamma mutations: clinical and molecular genetic study. Lancet 2004;364:875–882.
22. Bekheirnia MR, Zhang W, Eble T, et al. POLG mutation in a patient with cataracts, early-onset distal muscle weakness and atrophy, ovarian dysgenesis and 3-methylglutaconic aciduria. Gene 2012;499:209–212.